Intuition will be the originative source of scientific knowledge.

Posterior Analytics
Aristotle (AC 384-322)

Chapter 1

Introduction

The above quote is Aristotle's conclusion after formulating the two basic methods of scientific reasoning: induction and deduction (Aristotle, ∼AC 350)[1]. He formulated a scientific method consisting of staged deductions from premises to conclusions, starting from a primary premise. His argument was that the primary premise could only have been reached by induction apprehended (sparked) by intuition.

Almost all research in geophysics falls into one of two categories:

The first category consists of theory-driven research to develop a new theory or method, motivated by a desired result. Its merit is tested on experimental data to validate the new approach. The result is often binary; that is, it functions as pass-fail.

The second category consists of data-driven research to tackle and push experimental data, to observe novel phenomena. Results are difficult to predict until they appear at the end of a continuously evolving workflow. The results are diverse.

Any observational scientific study uses both inductive and deductive reasoning. But if I were to label the above two categories, I would argue that the first category reflects the deductive approach and the second category reflects the inductive approach. The study presented in this thesis falls in the second category.

[1]For a translation and commentary see Biondi (2004).

MOTIVATION

Seismic interferometry is a theory that predicts that the crosscorrelation of transmission responses at two stations retrieves a signal that resembles the recording made at one of the two stations as if the other station were a virtual source.

This technique has revolutionized how seismologists use surface waves to study the earth on a crustal scale. Prior to the retrieval of surface-wave Green's functions between two stations by noise interferometry, seismologist could only use wave-paths between earthquakes and receiver stations to image the earth. The limited spread of earthquakes provided a geographical constraint on imaging the earth. Now that surface-wave noise interferometry has become the leading method by which seismologists find surface-wave Green's functions, the Earth can be imaged at more places and at a higher resolution. However, at the onset of this study, little was known about the potential of surface-wave noise interferometry for reservoir-scale imaging.

Controlled-source seismic imaging is the dominant method by which geophysicists explore and monitor the subsurface for hydrocarbon exploration (Biondi, 2006). However, the extraction of hydrocarbons is a difficult operation that benefits from abundant information about the subsurface and from high-quality subsurface images. Controlled-source prospecting is routinely applied to monitor the subsurface for changes (Jack, 1997). However, even when a recording array is permanently installed a controlled-source surveying usually happens only once or twice a year. Ambient noise can be recorded continuously be permanently installed arrays. Green's functions extracted from noise may provide the opportunity for continuous imaging (even) in the absence of seismic shooting.

The research presented in this thesis is about seismic interferometry of microseism noise recorded by ocean-bottom cables installed over two fields in the Norwegian North Sea. I will show that the microseism noise does not illuminate the subsurface at the same frequencies and wavenumbers as controlled-source seismic prospecting does (Figure 1.1). Controlled-source data is dominated by reflections and refractions, and interface waves are excited only weakly. Ambient noise is dominated by fundamental

mode interface waves. Furthermore, the microseism frequency range ($0.175-1.75$ Hz) and controlled source frequency range ($2-60$ Hz) do not overlap and thus may provide complimentary information.

The near-surface is an imaging challenge (Butler, 2005). Knowledge of the near-surface helps to resolve wavefield imaging challenges at depth that are caused by near-surface transmission complexities (Cox et al., 1999). Recently, the applied seismology community has taken an interest in the use of surface waves for imaging of the near-surface, because Scholte waves have proven very sensitive to stresses in the near-surface and respond to near-surface geomechanical changes induced by hydrocarbon production at depth (Wills et al., 2008; Hatchell et al., 2009). Accurate knowledge of the near-surface may also help scientists to better understand geohazards involved with hydrocarbon exploration and production (Barkved, 2012; Landrøand Amundsen, 2011).

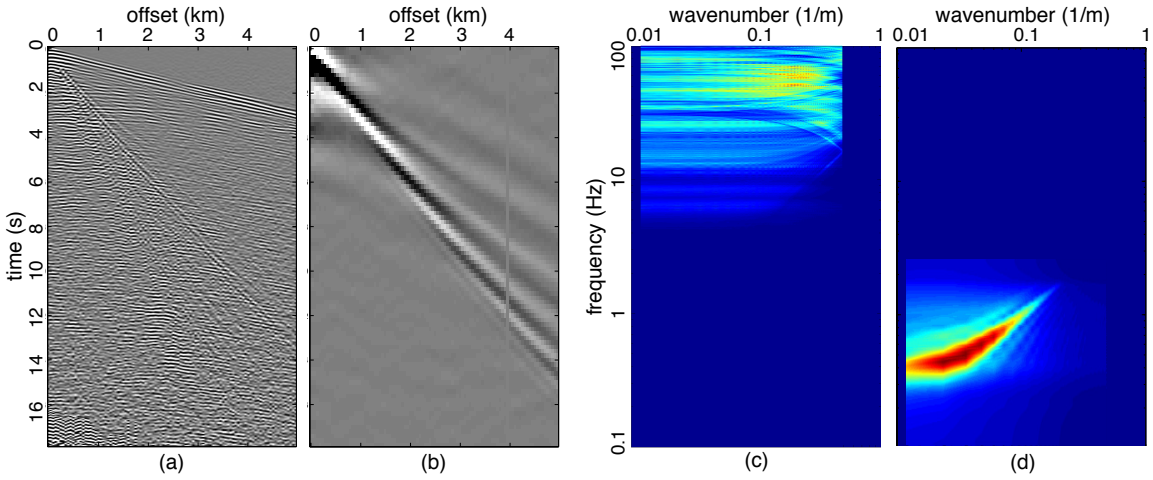

Figure 1.1: Offset gather of controlled-source data (a) and of virtual-source data (b) and their log-frequency versus log-wavenumber spectra in (c) and (d) respectively, courtesy BP. [**NR**] valhall-active-passive

BACKGROUND AND TERMINOLOGY

The terms controlled-source versus ambient-source seismology are used to distinguish the source energy under investigation (Figure 1.2). Exploration seismology conventionally prospects the subsurface using controlled sources such as airguns, vibrator-trucks or explosions (Telford et al., 1990). These prospecting techniques will be referred to as controlled-source methods, because the operators exert full control over the sources. The seismic-techniques that exploit seismic energy not directly controlled by the operators will be referred to as ambient-seismic methods. The terms active and passive seismics, also used in the discipline, misleadingly suggests that the ambient sources are somehow less active. These terms are also inappropriate when carried over from the exploration seismology community to the broader seismology community. Regional, crustal and global seismologists rarely use controlled-sources; a rare exception would be nuclear-source prospecting (Scheimer and Borg, 1984).

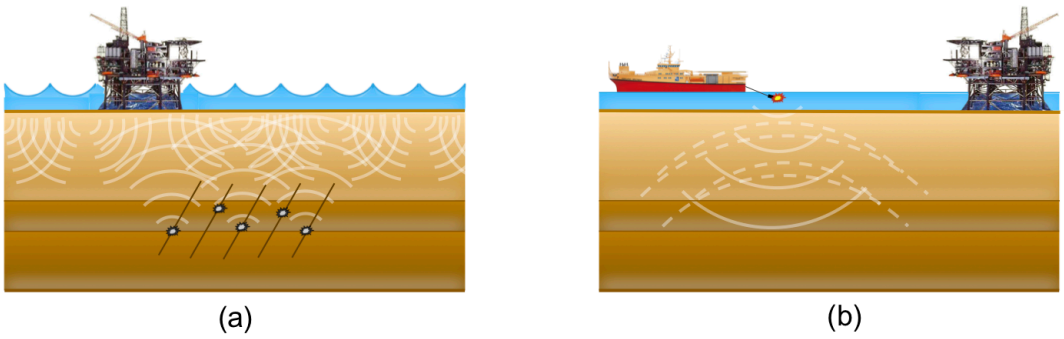

Figure 1.2: Ambient seismic (a) versus controlled seismic (b). [**NR**] ambient-vs-controlled

Studies of the the ambient seismic field can be categorized based on their philosophy of how to treat the ambient energy: deterministic versus non-deterministic. Although microseism and microseismic energy are often confused and used interchangeably in both the applied and non-applied seismology communities, the seismic energy has a completely different origin (Figure 1.3) in the two cases. Because microseism studies are rare in the exploration seismology community and microseismicity studies are rare in the earthquake seismology community, the similarity in terms

is often a source of confusion. In the exploration community, passive seismics commonly refers to studies of microseismic energy (Goodway, 2012; Shemeta et al., 2012). The source of microseismic energy is small earthquake-like events that are caused by, for example, hydraulic fracturing. These events excite a temporally and spatially sparse wavefield. This energy is studied deterministically for the source locations and wave-propagation paths between sources and receivers. The microseism energy composing the wavefields analyzed in this thesis, on the other hand, is excited by wind-generated ocean-waves (Longuet-Higgins, 1950). These waves interact to form pressure fluctuations on the sea floor and coast forming a spatial and temporally continuous excitation function exciting mostly interface waves. This energy can be studied non-deterministically for its spatial coherence (Aki, 1957) or deterministically for its excitation sources (Rhie and Romanowicz, 2006).

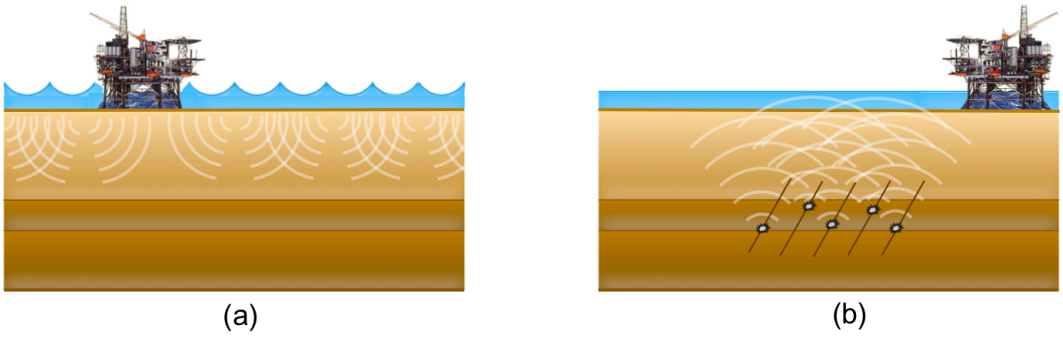

Figure 1.3: Microseisms (a) versus microseismicity (b). [**NR**] microseism-vs-microseismic

In this thesis I study microseism noise non-deterministically at an exploration scale. The term passive seismic interferometry (PSI) is well recognized by the community as utilizing ambient-seismic energy non-deterministically by crosscorrelation.

PASSIVE-SEISMIC INTERFEROMETRY

Crosscorrelations of ambient seismic recordings recorded at two stations, under favorable noise conditions, yield an Estimated Green's Function (EGF). The crosscorrelation turns noise into signal as if one of the stations acted as a seismic source because there was no real source at that station. This station becomes a virtual seismic source. Thus, PSI provides a means to continuously survey the subsurface in the absence of seismic shooting.

Aki (Aki, 1957) first derived (from a modal formulation) how to retrieve the dispersion of surface waves from the crosscorrelations of a circle of stations. Claerbout (1968) derived that the one dimensional auto-correlation of transmission responses would yield the reflection response (using 1D reciprocity theorems) and conjectured an extension to three-dimensions by crosscorrelations. This conjecture was used by Cole (1995) for seismic data and Rickett and Claerbout (1999) for helioseismology data. This was formally proven for the elastodynamic case by Lobkis and Weaver (2001); Weaver and Lobkis (2002) based on normal mode expansions and by Wapenaar (2003, 2004); Wapenaar and Fokkema (2006) using 3D reciprocity theorems.

This theory and the consequent crosscorrelation technique has been applied in solar physics (Duvall Jr. et al., 1993; Rickett and Claerbout, 1999), in laboratory acoustics (Weaver and Lobkis, 2001, 2002), and very extensively in crustal-scale seismology starting with (Campillo and Paul, 2003; Shapiro and Campillo, 2004). Baskir and Weller (1975); Scherbaum (1987); Cole (1995); Daneshvar et al. (1995) were amongst the first to test Claerbout's relationship between the reflection response and the autocorrelation of the transmission response at an reservoir-scale. Efforts to retrieve body-wave energy have proven to be challenging. The successes of seismic interferometry on a crustal scale led to a resurgence of research in exploration-scale body-wave seismic interferometry attempts (Artman, 2007; Draganov, 2007; Draganov et al., 2009; Ruigrok et al., 2011; Edme and Halliday, 2011; Ruigrok and Wapenaar, 2012).

Meanwhile there were a few attempt at exploration-scale surface-wave interferometry. Prior to the study presented in this thesis, Stewart (2006) retrieved Scholte waves

from an Ocean-Bottom Cable (OBC) recording of microseism noise in the Gulf of Mexico. In the following years, Dellinger and Yu (2009) retrieved Scholte-waves from microseism-noise between $0.3-3$ Hz recorded by OBCs at Valhall field in the North Sea and Bussat and Kugler (2009) retrieved two Scholte-wave modes and an acoustic guided mode from microseism noise between $0.15-1.5$ Hz recorded by Ocean-Bottom Nodes (OBNs) at Astero field in the North Sea. Landès et al. (2009) retrieved Love wave using platform noise between $3-30$ Hz at Valhall. De Ridder and Biondi (2010) retrieved Rayleigh waves between $1-7$ Hz using anthropogenic noise recorded on land in Saudi Arabia.

Theory

The basic result of seismic interferometry between two seismic recordings, $r(\mathbf{x}_b)$ and $r(\mathbf{x}_a)$, made at $\mathbf{x}_b$ and $\mathbf{x}_a$ is described by the following expression:

$$\Big\langle r(\mathbf{x}_b,t) \otimes r(\mathbf{x}_a,-t) \Big\rangle \approx \oint_{\mathbf{x}_s} G(\mathbf{x}_b,\mathbf{x}_s,t) \otimes G(\mathbf{x}_a,\mathbf{x}_s,-t) \propto G(\mathbf{x}_b,\mathbf{x}_a,t) + G(\mathbf{x}_a,\mathbf{x}_b,-t), \tag{1.1}$$

where $\langle\rangle$ denotes a spatial ensemble average over source responses surrounding the receiver pair. The source positions are denoted x_s which is the integration variable in the second term. $G(\mathbf{x}_b,\mathbf{x}_a,t)$ denotes the Green's function recorded at $\mathbf{x}_b$ as a response to an impulse source at $\mathbf{x}_a$. $G(\mathbf{x}_a,\mathbf{x}_b,-t)$ denotes the reciprocal time-reverse Green's function recorded at $\mathbf{x}_a$ as a response to an impulsive source at $\mathbf{x}_b$. Crosscorrelation is denoted by convolution, $\otimes$, between two time-series with one series being time-reversed. For simplicity the source spectrum in the ambient seismic recordings field is omitted. Equation 1.1 expresses that under favorable circumstances, the crosscorrelation of seismic recordings made at $\mathbf{x}_b$ and $\mathbf{x}_a$ evaluates a sum of crosscorrelations of many observed responses of sources surrounding the receiver pair. Equation 1.1 also expresses that the evaluation of this sum is proportional to the sum of the Green's function from $\mathbf{x}_a$ to $\mathbf{x}_b$ and its time-reversed reciprocal (also named the homogeneous Green's function). Appendix A contains a more extensive derivation of the result of seismic interferometry for elastodynamic wavefields. This derivation starts from a

Green's function representation that is based on the principle of energy conservation (Wapenaar and Fokkema, 2006).

The first assumption for Green's function retrieval by crosscorrelation is that the energy flux in the ambient wave field is equipartitioned; i.e., energy flux is independent of direction, and all wave modes are excited equally (Lobkis and Weaver, 2001). Modal-energy equipartition alone is insufficient (Snieder et al., 2010). We require that sources surrounding the station pair be uncorrelated so that the crosscorrelation of a long recording time evaluates an ensemble average of the independent contributions of the sources surrounding the station pair (Wapenaar and Fokkema, 2004, 2006).

Example scenarios

To illustrate the remarkable result predicted by Equation 1.1, I present examples of seismic interferometry in the presence of three different source distributions. Figure 1.4(a) shows a receiver pair, A and B, that is completely surrounded by sources. Figure 1.4(b) shows a correlation-gather of the individual crosscorrelations of each source and the result of summing all crosscorrelations (blue curve). In this ideal situation, the sum of all crosscorrelations perfectly matches the homogeneous Green's function (red-dashed curve). Sources in two regions (indicated in Figure 1.4(a) by gray shading) provide leading contributions to the total sum of the crosscorrelations. Crosscorrelated energy of those sources arrives with the correct travel-time but the wrong phase of the Green's function between A and B (Snieder, 2004). These regions are referred to as stationary-source regions (Snieder, 2004). This region is defined along two ray-paths emitted from A and B that hit station B and A respectively and extend outward.

Figure 1.5(a) shows a receiver pair A and B that is not completely surrounded by sources. There are no sources in the stationary phase region for the causal portion of the homogeneous Green's function; the source distribution ends abruptly on either side. In the upper-right area, sources grew weaker on either side of another region with no sources. Furthermore, one source located below the stations is much stronger than

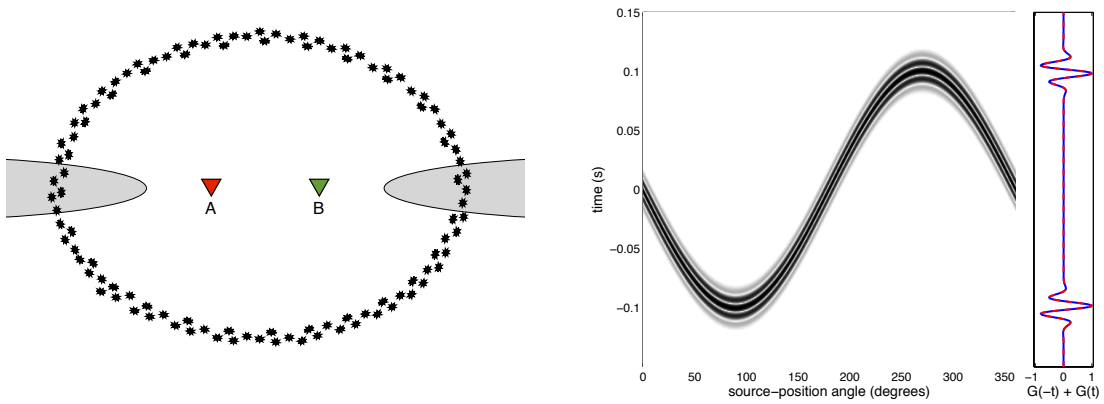

(a) (b)

Figure 1.4: a) Schematic of an ideal source distribution for passive seismic interferometry. b) Correlation gather as a function of source-position angle (clockwise with the vertical) plus retrieved (blue curve) and directly computed (red dashed) Green's functions. [**NR**] [**ER**] si-ideal,si-example-1

the other sources. Figure 1.5(b) shows a correlation gather of the individual crosscorrelations of each source, and the result of summing all crosscorrelations (blue curve). In this example, the retrieved result only partially matches the homogeneous Green's function (red-dashed curve). The anticausal portion of the homogeneous Green's function is well retrieved because the sources covered the stationary-phase region of the Green's function from B to A. However, the causal portion of the homogeneous Green's function is not retrieved because of a lack of sources in the stationary-phase region for the Green's function from B to A. The abrupt ends of the source distribution on either side of the stationary-phase region cause spurious energy to arrive before the arrival time of the Green's function from A to B. If the source distribution did not end abruptly, almost no spurious event would have arisen in the crosscorrelation result. When one source is considerably stronger than the other sources, the result is a spurious event in the crosscorrelation result.

The resulting crosscorrelation of an imperfect source distribution is assymetric. Symmetry is often used as a quality factor of noise crosscorrelations, however symmetry is not a conclusive quality factor. Figure 1.6(a) shows a source distribution that,

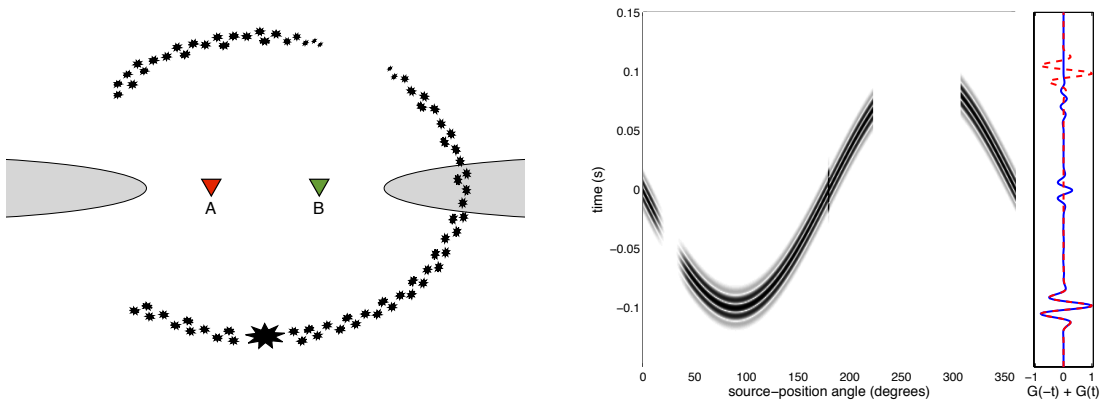

(a) (b)

Figure 1.5: a) Schematic of a realistic imperfect source distribution for passive seismic interferometry. b) Correlation gather as a function of source-position angle (clockwise with the vertical) plus retrieved (blue curve) and directly computed (red dashed) Green's functions. [**NR**] [**ER**] si-real,si-example-2

under certain circumstances, may lead to a perfectly symmetric yet completely wrong crosscorrelation result. There are no sources in either stationary-phase region, but due to the symmetry in their source-position in a medium with no velocity variation, the energy in causal and anti-causal windows arrived at the same correlation lag.

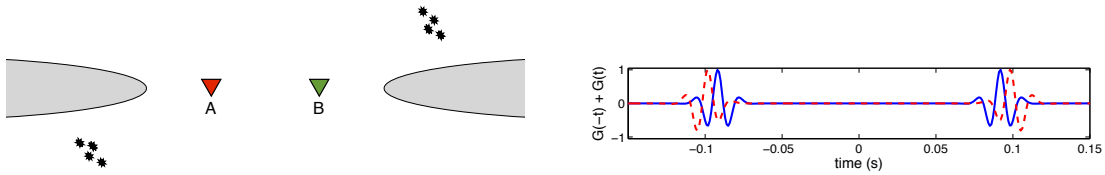

(a) (b)

Figure 1.6: a) Schematic of a source-distribution in which the symmetry condition fails as quality control. b) Retrieved (blue curve) and directly computed (red dashed) Green's functions. [**NR**] [**ER**] si-symfail,si-example-3

The symmetry constraints on the source distributions required for the scenario in Figure 1.6(a) and 1.6(b) to occur may be impossible to satisfy in a complicated medium with velocity variations. Thus, symmetry is generally a safe quality constraint. However, from the second scenario we see that it is also too strict of a quality

factor. The crosscorrelation may be weak or lack energy in the causal portion, yet it may match the Green's function perfectly in the anticausal portion (or vice versa).

Correlation processing

There are several choices for preprocessing and correlation functions for passive-seismic interferometry. First, dominant arrivals such as teleseismic events and earthquakes are commonly removed. Because the transient nature of the ambient seismic field and local site effects make straightforward Green's Function extraction by cross spectra difficult, authors of early successful noise correlations studies applied a time-domain normalization by sign-bit (Campillo and Paul, 2003; Sabra et al., 2005a). Sign-bit normalization is a crude processing tool, and later authors used a daily RMS average clipping threshold (Shapiro et al., 2005) or a running normalization (Bensen et al., 2007). Several frequency-domain normalizations were proposed to mitigate the signature of the power spectrum of the noise sources: deconvolution (Vasconcelos and Snieder, 2008b,a), cross coherence (Prieto et al., 2009a) or multitaper cross spectral analysis (Prieto et al., 2009b). More recently, combinations of time-domain and frequency-domain normalizations were proposed by adaptive filtering (Kimman, 2011; Hadziioannou et al., 2011) based on time-frequency decomposition of the signal by analytical S-transform (Dziewonski et al., 1969; Stockwell et al., 1996) or based on Welch's method (Seats et al., 2012). Welch's method (Welch, 1967) computes and averages power-spectra over overlapping windows. When crosscorrelating the microseism noise recorded at Valhall (Chapter 3), I computed straightforward cross spectra under half-hour overlapping windows (similar to Welch's approach). These cross spectra could, if needed, still be whitened before stacking. When crosscorrelating the microseism noise recorded at Ekofisk (Chapter 6), I computed straightforward cross spectra under 4-hour windows.

SURFACE-WAVE GROUP AND PHASE TOMOGRAPHY

The first successes of surface-wave retrieval by seismic interferometry were immediately followed by tomography studies on regional and continental scales (Sabra et al., 2005b; Shapiro et al., 2005; Yao et al., 2006; Moschetti et al., 2007; Lin et al., 2007; Bensen et al., 2008) and many more. Surface-wave velocity tomography has traditionally aimed at creating maps of phase and group velocities. Wielandt (1993) discussed the difference between the observed phase-velocity that depends on the local geometry of the wavefield and the phase-velocity parameter in the wave equation. Scattering and bending of surface waves off heterogeneities modify the observable phase of the wavefield into an apparent-phase velocity. But the relationship between apparent phase or group velocities to three-dimensional structures is not straight forward.

Ray theory is inadequate to describe wave propagation in the vicinity of lateral heterogeneities of the order of a wavelength or smaller (Snieder, 2002). But the weighted average of the phase and group-velocities of a set of forward scattered waves, to first order, are representative of the the Fresnel zone of a single wave through a reference medium (Snieder and Lomax, 1996). This explains why ray-based tomography performs well even in media with anomaly sizes of the order of a wavelength. One way to avoid this discrepancy is by using finite-frequency sensitivity kernels (Zhou et al., 2004). There is discussion whether finite-frequency kernels offer benefits over ray theory for surface waves (Sieminski et al., 2004; Trampert and Spetzler, 2006). For a dense station network the use of finite-frequency kernels is expected to offer an improvement over ray theory, especially when the anomalies are of the order of a wavelength (Yang and Forsyth, 2006). Finite-frequency effects for noise-correlations (Tromp et al., 2010) are omitted in this thesis but may be an interesting avenue for future research pursuits. Another property of my tomography problem that bodes well for the spatial resolution is the dense station coverage. A tomography of global travel-times will, due to the dense coverage of travel-time paths, implicitly carry information about the gradient of travel-time surfaces. This gradient maps directly into local slowness as per the eikonal equation. This is explicitly used by eikonal or Helmholtz tomography (Lin et al., 2009; Lin and Ritzwoller, 2011).

THESIS OVERVIEW

There are eight chapters in this thesis. In the four chapters after the introduction I analyze multiple datasets recorded at Valhall. In the sixth chapter I analyze a dataset from Ekofisk. Studying a second field provides insight into which observations made at Valhall and Ekofisk may be generalized to other OBC arrays. For both datasets I use a similar workflow to explore the characteristics of the recorded microseism noise before I create virtual seismic sources by crosscorrelation. I perform straight-ray group-velocity tomography for Love and Scholte waves at Valhall and for Scholte waves at Ekofisk. In the seventh chapter I introduce a formulation of eikonal tomography for elliptically anisotropic surface-wave phase velocities. This technique is applied to Scholte and Love waves at Valhall and Scholte waves at Ekofisk. The conclusions and contributions of this thesis are summarized in chapter eight.

Chapter 1: Introduction

This chapter; containing an introduction and overview of the thesis.

Chapter 2: Characterization of microseism noise

The basis for successful application of passive seismic interferometry depends on the characteristics of the ambient noise. This chapter provides a unique analysis of the character of microseism noise as recorded by a dense array. I start by introducing four datasets recorded at Valhall field in the Norwegian North Sea in 2004, 2005, 2008 and 2010. The microseism energy recorded at frequencies between between 0.175 and 1.75 Hz is characterized by studying its spectral amplitude as a function of time and space. The propagation direction of the microseism noise is further characterized by beam steering.

Chapter 3: Crosscorrelation of microseism noise

The microseism noise in the 2004, 2005 and 2010 recordings made at Valhall and introduced in Chapter 2 are crosscorrelated and I construct virtual-seismic sources as predicted by seismic interferometry. Crosscorrelating all component combinations between the 3-component geophones of two stations retrieves a full virtual-seismic source matrix. These virtual-source matrices are retrieved for each station-pair in Valhall's LoFS array and transformed to a cylindrical coordinate system centered around each virtual source. The crosscorrelations are analysed for their convergence rate towards a long-term average. And finally I perform a mode-analysis of the wave types emitted by the virtual seismic sources by creating dispersion images.

Chapter 4: Group-velocity tomography at Valhall

The virtual-seismic sources computed in Chapter 3 are imaged by group-velocity tomography. Traveltimes picked on vertical-to-vertical crosscorrelation are inverted for Scholte wave group-velocity images. Traveltimes picked on transverse-to-transverse crosscorrelation are inverted for Love wave group-velocity images. The temporal resolution of a map based on a particular stack length is estimated by the standard deviation between several realizations from independent data. The regularization strength is normalized for all inversions of traveltime picks from crosscorrelations of a particular stack length. To verify this, the variation between inverted maps based on a particular stack length, for the maps from the datasets recorded in 2004, 2005 and 2010, is quantified as a function of regularization strength.

Chapter 5: Time-lapse group-velocity images at Valhall

Almost seven years passed between the recordings in 2004 and 2010. It is known from repetitive controlled-source surveying that production and development of Valhall's reservoir affected velocities in the shallow subsurface (Wills et al., 2008; Zwartjes et al., 2008; Hatchell et al., 2009). In this chapter, I compute time-lapse Scholte-wave

images obtained from ambient noise by differentiating sets of tomographic images, based on particular stack lengths, from the recordings in 2004, 2005 and 2010. I will determine the statistical significance of the computed time-lapse images by a Welch's t-test between the sets of velocity estimates.

Chapter 6: Ambient seismic noise tomography at Ekofisk

In Chapter 6 I study an almost 40-hour recording from the Life of Field Seismic (LoFS) array installed over Ekofisk field to evaluate the opportunities of passive seismic interferometry at a second field. The correlation analysis and group-velocity tomography undertaken in Chapters 2 to 4 on Valhall microseism noise recorded by geophones is repeated for microseism noise recorded by pressure sensors at Ekofisk.

Chapter 7: Elliptically anisotropic eikonal tomography

I present a novel method for anisotropic eikonal tomography that inverts for elliptically anisotropic phase-velocities from spatial derivatives of traveltime surfaces. The parameters of the ellipse are inverted from two perpendicular spatial derivatives of traveltime surfaces. The novelty of this anistropic formulation is that it is based on an elliptically anisotropic wave equation, instead of on an anisotropically interpreted isotropic wave equation. Another major advantage is that the inverted anisotropic phase-velocities can be regularized over space and frequency. The method is applied to Scholte and Love waves at Valhall and on Scholte waves at Ekofisk.

Chapter 8: Conclusions

I summarize the most important results in this dissertation.

Appendices

There are four appendices to this dissertation. In Appendix A I present a derivation for the equations for seismic interferometry in the particular case of buried ocean-bottom cable (OBC) recordings. In Appendix B I summarize the discrete Fourier transformation and definitions of amplitude, power and cross spectra as used in ocean acoustics. In Appendix C I compute the geophone transfer functions for Valhall. In Appendix D I present all Scholte wave group-velocity maps (for 2004, 2005 and 2010) for two central frequency ranges, $0.75 - 0.95$ Hz and $1.35 - 1.55$ Hz, based on 6-, 12-, 24-, 60- and 120-hour non-overlapping stacks.

ACKNOWLEDGMENTS

My thanks to BP and the partners of the Valhall Field (BP Norge and Hess Norge) for permission to publish the data in this chapter. I would like to thank the founders, developers and authors of Wikipedia, their pages have been an a invaluable tool throughout my studies and research. Wikipedia also proved an endless and enjoyable source for procrastinative reading. I would like to thank Kathryn Hume for a brief reflection on my opening paragraphs. One of the aspects that confirm the accuracy of the results presented in this thesis and obtained from ambient-seismic noise is the comparison with results obtained from controlled-source data or other measurements. I am grateful to BP America, BP Norge AS, Hess Norge AS, ConocoPhillips, Shell, ConocoPhillips Skandinavia AS, Total E&P Norge AS, ENI Norge, Statoil Petroleum AS and Petoro AS, for releasing these controlled-source images and data to me. I am particularly grateful to Damien Dieulangard who went through the trouble of making the offset gather and frequency-wavenumber spectrum of controlled-source data presented in this chapter while he was in the middle of a move across the North Sea.